Altered expression of ganglioside GM3 molecular species and a potential regulatory role during myoblast differentiation

Shinji Go[‡1], **Shiori Go**[‡§1], **Lucas Veillon**[‡], **Maria Grazia Ciampa**[¶], **Laura Mauri**[¶], **Chihiro Sato**[§], **Ken Kitajima**[§], **Alessandro Prinetti**[¶], **Sandro Sonnino**[¶], and **Jin-ichi Inokuchi**[‡2]

From the ‡*Division of Glycopathology, Institute of Molecular Biomembrane and Glycobiology, Tohoku Medical and Pharmaceutical University, Sendai 981-8558, Japan, §Bioscience and Biotechnology Center, Nagoya University, Nagoya 464-8601, Japan, and ¶Department of Medical Biotechnology and Translational Medicine, University of Milan, 20090 Segrate Milano, Italy*

Edited by Gerald W. Hart

Gangliosides (sialic acid-containing glycosphingolipids) help regulate many important biological processes, including cell proliferation, signal transduction, and differentiation, via formation of functional microdomains in plasma membranes. The structural diversity of gangliosides arises from both the ceramide moiety and glycan portion. Recently, differing molecular species of a given ganglioside are suggested to have distinct biological properties and regulate specific and distinct biological events. Elucidation of the function of each molecular species is important and will provide new insights into ganglioside biology. Gangliosides are also suggested to be involved in skeletal muscle differentiation; however, the differential roles of ganglioside molecular species remain unclear. Here we describe striking changes in quantity and quality of gangliosides (particularly GM3) during differentiation of mouse C2C12 myoblast cells and key roles played by distinct GM3 molecular species at each step of the process.

Glycosphingolipids (GSLs)[3] are constituents of eukaryotic cell membranes located exclusively on the outer leaflet of the plasma membrane. Gangliosides, a subgroup of GSLs having one or more sialic acid residues, are involved in regulation of numerous cell biological events, including development, trafficking, signaling, and cellular interactions. Gangliosides have pathophysiological functions in diseases such as cancer, neurodegenerative disorders, and diabetes (1, 2). Sialic acid plays a key role in the biological activities of gangliosides (3). For example, we demonstrated that localization of insulin receptor in caveolae is disrupted by elevated levels of endogenous GM3 during the state of insulin resistance. This effect is due to electrostatic interaction between the lysine residue of insulin receptor (Lys-944) and the carboxyl group of sialic acid of GM3 (4–8).

The structural diversity of GSLs arises from both the ceramide (Cer) moiety and glycan portion (Fig. 1). Cer is composed of sphingosine and a single acyl chain (Fig. 1B). Cer acyl chains vary in length of carbon backbone, degree of saturation, and the presence/absence of α-hydroxylation (9, 10).

Additional structural diversity of gangliosides arises from sialic acid (acidic sugar molecule with characteristic nine-carbon backbone) in the glycan portion. The most common sialic acid in mammals is N-acetylneuraminic acid (Neu5Ac). The other common sialic acid, N-glycolylneuraminic acid (Neu5Gc), differs from Neu5Ac by the presence of an additional oxygen atom in the acyl group at position C5 (Fig. 1B). Further structural diversity of sialic acids results from combinations of this variation at position C5 with modifications of hydroxyl groups at positions C4, C7, C8, and C9 by acetate, lactate, sulfate, phosphate esters, or methyl ethers. Sialic acid modifications greatly alter the size, hydrophobicity, net charge, and enzymatic susceptibility of the parent compound (11). Such structural divergence generated by different combinations of Cer and sialic acids in gangliosides (Fig. 1B) results in a huge numbers of "molecular species." The identity of sialic acid species in GM3 affects its biological properties. GM3 inhibits EGFR-tyrosine kinase to differing degrees depending on its sialic acid species. Such a difference apparently results from differential carbohydrate-carbohydrate interactions between EGFR and GM3 (Neu5Ac) or GM3 (Neu5Gc) (12). We have also demonstrated relationships between various metabolic diseases and levels of serum ganglioside GM3 "acyl chain" molecular species. In particular, levels of GM3 with hydroxylated acyl chain species in human serum show strong correlations with several risk factors for metabolic diseases (13).
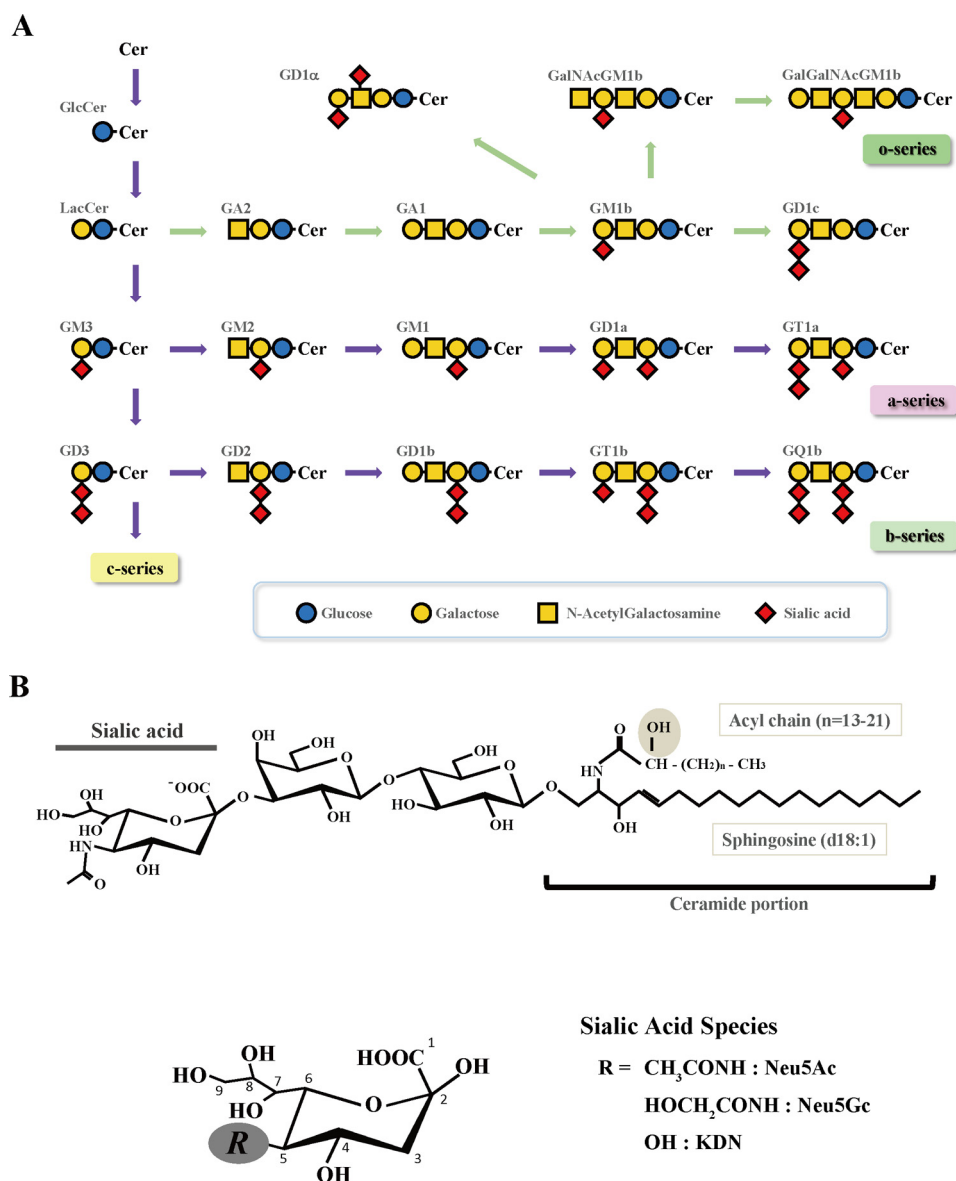
Taken together, the above findings indicate that differing molecular species of a given ganglioside have distinct biological properties and regulate specific and distinct biological events. Elucidation of the function of each molecular species is important and will provide new insights into ganglioside biology.

[1] Both authors contributed equally to this study.

[2] To whom correspondence should be addressed: Division of Glycopathology, Institute of Molecular Biomembrane and Glycobiology, Tohoku Medical and Pharmaceutical University, 4-4-1, Komatsushima, Sendai 981-8558, Japan. Tel.: 81-22-727-0117; Fax: 81-22-727-0076; E-mail: jin@tohoku-mpu.ac.jp.

[3] The abbreviations used are: GSL, glycosphingolipid; Cer, ceramide; CerS, ceramide synthase; Neu5Ac, N-acetylneuraminic acid; Neu5Gc, N-glycolylneuraminic acid; EGFR, EGF receptor; MyHC, myosin heavy chain; HPTLC, high performance thin layer chromatography; CMAH, CMP-Neu5Ac hydroxylase; Elovl, expression levels of fatty acyl-CoA elongase; DM, differentiation medium; GM3, Siaα2,3Galβ1,4Glc-ceramide; GM2, GalNAcβ1,4(Siaα2,3)Galβ1,4Glc-ceramide; GM1, Galβ1,3GalNAcβ1,4(Siaα2,3)Galβ1,4Glc-ceramide; GD1a, Siaα2,3 Galβ1,3GalNAcβ1,4(Siaα2,3)Galβ1,4Glc-ceramide.

ASBMB

Figure 1. Structural diversity of gangliosides. *A*, ganglioside biosynthetic pathways. *B*, structures of ganglioside GM3 and sialic acid molecular species.

Regulation of skeletal muscle formation is an essential process in both normal development and repair of damaged muscle tissue. Differentiation of skeletal muscle cells (myocytes) is a multistep process; the steps include signal transduction, cell adhesion, and cell-cell fusion (14, 15). Gangliosides are known to modulate various plasma membrane functions, *e.g.* cell-cell interactions, signal transduction, and membrane ion channel activity, through formation of functional membrane microdomains termed "rafts." Gangliosides are presumably involved in these processes in myocytes (16–19); however, direct evidence for such involvement is limited and fragmentary. In the present study we evaluated expression of gangliosides in myoblasts during differentiation. We observed striking changes in ganglioside molecular species composition during differentiation and assessed their differential functions. GM3 (Neu5Gc) and 16:0 acyl chain species, in particular, appear to play essential roles in differentiation of myoblasts to myotubes.

Results

Changes in ganglioside quantity and quality during myogenic differentiation

C2C12 is a myoblast line established from normal adult C3H mouse leg skeletal muscle and is a well established model of *in vitro* differentiation. C2C12 cells were cultured to ~90% confluence in growth medium and then cultured in differentiation medium (DM; see "Experimental procedures"). Upon differentiation stimulus, the cells gradually fused to form multinucleated fibers (myotubes) (Fig. 2*A*) as expected. Differentiation to myotubes was confirmed by Western blotting. Levels of differentiation marker proteins myogenin and myosin heavy chain (MyHC) increased during differentiation (Fig. 2*B*). HPTLC revealed the appearance of bands corresponding to GM3, GM2, GM1, and GD1a mobilities during differentiation (Fig. 2*C*). Amounts of all acidic GSLs increased gradually during differentiation (Fig. 2*C*). In particular, GM3 content increased strik-
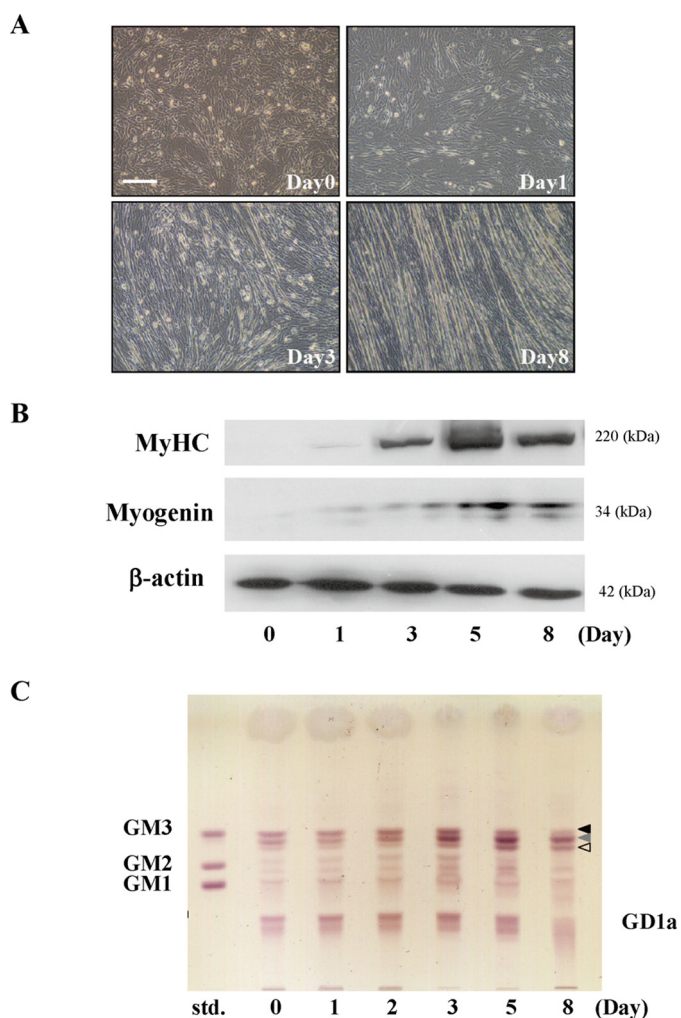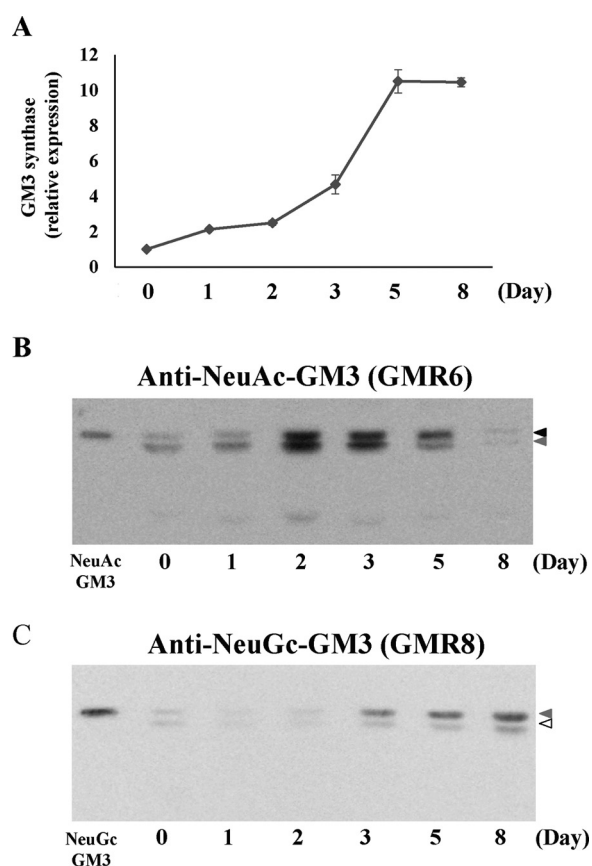
Figure 2. Changes of ganglioside expression during myoblast C2C12 differentiation. Differentiation of C2C12 cells was induced by culture in DM (see "Experimental procedures"). *A*, morphology of proliferating cells (day 0) and myotube formation on days 2–8, as revealed by phase-contrast microscopy. *Scale bar*, 200 μm. *B*, expression of differentiation marker proteins myogenin and MyHC on various days, revealed by Western blotting. β-actin: loading control. Shown are representative Western blot images. *C*, GSL fraction was prepared as described under "Experimental procedures." Acidic GSLs extracted from cells (0.2 mg protein basis) were spotted and separated on HPTLC. GSLs were visualized by orcinol/sulfuric acid staining. Pointers indicate GM3 species with differing polarity (see "Changes in ganglioside quantity and quality during myogenic differentiation" under "Results"). Shown is a representative HPTLC image.

Figure 3. Alteration of sialic acid species of GM3 during C2C12 differentiation. *A*, the GM3 synthase mRNA expression levels on the indicated days, determined by quantitative RT-PCR. Data represent the relative gene expression in cells of each day compared with that in cells of day 0 (set to 1.0 separately for each target gene). Average -fold change was obtained from three experiments, shown as the means $\pm$ S.D. *B*, GM3 (Neu5Ac) expression, detected by TLC immunostaining with specific mAb GMR6. *C*, GM3 (Neu5Gc) expression, detected by TLC immunostaining with specific mAb GMR8. Pointers indicate the position of the GM3 band on HPTLC in Fig. 2.

ingly, with three major bands. Through day 2, the top band (*black pointer*) and middle band (*gray pointer*) were the major GM3 bands. From day 3 onward, the top band decreased, and the middle band and bottom band (*white pointer*) became the major bands. These findings revealed clear changes in quantity and quality of GM3 molecular species, reflecting their importance in myogenic differentiation.

Changes of sialic acid species in gangliosides during myogenic differentiation

GM3 synthase expression increased during differentiation (Fig. 3*A*), consistent with the observed increase of GM3 levels (Fig. 2*A*). To evaluate ganglioside changes during differentiation, we used TLC immunostaining and fluorometric HPLC to assess the quantity and quality of lipid-linked sialic acids.

Changes of sialic acid species of GM3 were confirmed by TLC immunostaining using specific anti-GM3 mAbs. For anti-GM3 (Neu5Ac) mAb GMR6, positive staining was detected at day 0, and its intensity increased until day 3 and decreased thereafter (Fig. 3*B*). In contrast, for anti-GM3 (Neu5Gc) mAb GMR8 (20), positive bands were very weak until day 2 then increased gradually after day 3 (Fig. 3*B*). High GM3 (Neu5Gc) expression was maintained even on day 8.

Quantity and quality of lipid-linked sialic acids were next assessed by fluorometric HPLC. In C2C12 myoblasts before differentiation, almost all gangliosides contained Neu5Ac as sialic acid in the glycan portion (Fig. 4*A*, ■). After differentiation induction, the total amount of lipid-linked sialic acid increased (Fig. 4*A*, ▲), consistent with TLC immunostaining results (Fig. 2*C*). The amount of lipid-linked Neu5Ac increased gradually through day 3 and declined thereafter. In contrast, lipid-linked Neu5Gc was barely detectable until day 2, increased markedly on day 3, and by day 5 was the major sialic acid species (Fig. 4*A*, ▲), again consistent with TLC results (Fig. 3, *B* and *C*). Taken together, these findings demonstrate that sialic acid species of gangliosides change from Neu5Ac to Neu5Gc during myogenic differentiation of C2C12 cells.
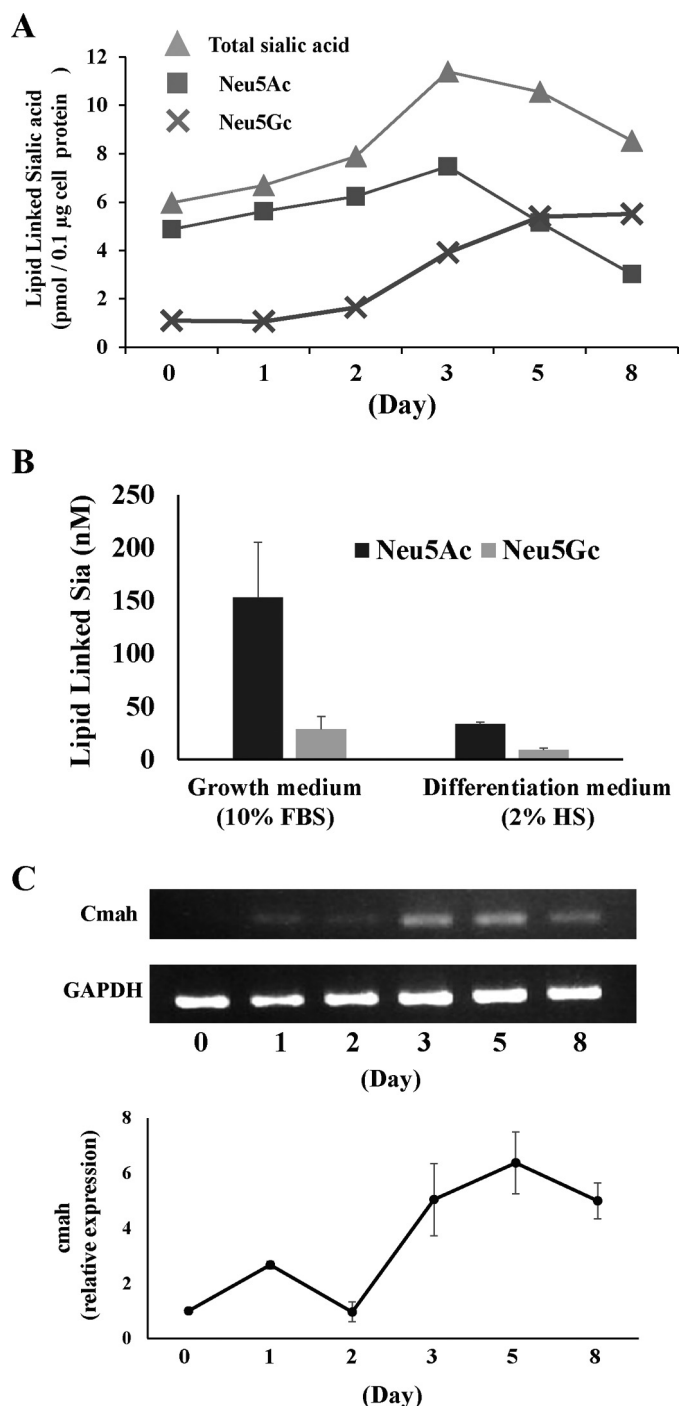
Figure 4. Quantitative and qualitative analysis of lipid-linked sialic acid species during C2C12 differentiation. *A*, lipid-linked sialic acid species in C2C12 were quantified and qualified by fluorometric HPLC. ▲, total lipid-linked sialic acids. ■, lipid-linked Neu5Ac. ×, lipid-linked Neu5Gc. Detected sialic acids: sum of sialic acids in GM3, GM2, GM1, and GD1a. *B*, lipid-linked sialic acid species in growth and differentiation medium were quantified by fluorometric HPLC. Shown is growth medium containing 10% FBS (*black bar*) and differentiation medium containing 2% HS (*gray bar*). *C*, expression levels of *Cmah* mRNA, determined by agarose gel electrophoresis and quantitative RT-PCR. Data represent the relative gene expression in cells of each day compared with that in cells of day 0 (set to 1.0 separately for each target gene). Average -fold change obtained from three experiments is shown as the means ± S.D.

Neu5Gc residues on glycans are synthesized from CMP-Neu5Gc through catalytic activity of sialyltransferases. There are two CMP-Neu5Gc synthesis pathways in mammalian cells. (i) In the salvage pathway, cells take up extracellular Neu5Gc-containing glycoconjugates derived from foods such as meat, fish, and eggs (or from serum in the case of cultured cell lines). Subsequently, Neu5Gc-containing glycoconjugates are hydrolyzed to Neu5Gc monosaccharides in lysosomes. Neu5Gc monosaccharides are transported to cytosol, and Neu5Gc is activated to CMP-Neu5Gc by CMP-sialic acid synthetase in the nucleus (21–23). (ii) In the *de novo* synthesis pathway, sialic acid Neu5Ac is synthesized in cytosol and activated to CMP-Neu5Ac in the nucleus, and CMP-Neu5Ac is subsequently converted to CMP-Neu5Gc by the enzyme CMP-Neu5Ac hydroxylase (CMAH) in cytosol (24, 25). CMP-Neu5Gc is transported into the Golgi apparatus, where it undergoes transfer to glycans through catalytic activity of various sialyltransferases. Reverse-transcription polymerase chain reaction (RT-PCR) analysis of the CMAH encoding gene (*Cmah*) revealed that expression level of *Cmah* mRNA was very low during days 0–2 but increased thereafter (Fig. 4*C*). Expression of *Cmah* mRNA was correlated with GM3 (Neu5Gc) level during C2C12 differentiation (Figs. 3 and 4).

It is known that fetal bovine and horse serum contain Neu5Gc glycoconjugates. Therefore, we analyzed sialic acid in growth (10% FBS) and differentiation (2% HS) medium and confirmed the existence of Neu5Gc in both mediums. Lipid-linked Sia in the media is shown in Fig. 4*B*. Growth medium contained large amounts of sialyl glycosphingolipids compare with differentiation medium. Both mediums contained large amounts of Neu5Ac compare with Neu5Gc. Although Neu5Gc glycosphingolipids, especially Neu5Gc-GM3 in medium, may be taken up and utilized by differentiating cells, the amounts would be small. Because the expression levels of both GM3 synthase and *Cmah* increased after the induction of differentiation (Figs. 3*A* and 4*C*), we could conclude that the increase of Neu5Gc-GM3 during differentiation may be due to the increased *de novo* synthesis.

Changes of acyl chain structures in the Cer portion of GM3 during myogenic differentiation

Structural diversity of GM3 derived from acyl chain structures in C2C12 cells was evaluated by LC-MS/MS after differentiation induction. On day 0 (Fig. 5*A*, *black bars*), the three most abundant GM3 species detected were Neu5Ac-GM3 (d18:1–24:0), Neu5Ac-GM3 (d18:1–24:1), and Neu5Ac-GM3 (d18:1–16:0). Species with acyl chain carbon number 24 accounted for >50% of total GM3 (Fig. 5*B*, *green* and *blue colors*). Species that were abundant on day 0 contained primarily Neu5Ac as sialic acid, consistent with TLC immunostaining and HPLC results (Figs. 3 and 4).

On day 7, when differentiation was completed, Neu5Gc-GM3 (d18:1–16:0) was the most abundant GM3 molecular species, and Neu5Ac-GM3 (d18:1–16:0) was the second most abundant (Fig. 5*A*). GM3 species with 16:0 acyl chains accounted for ~70% of the total. Proportions of Neu5Ac species were lower, and those of Neu5Gc species were higher on day 7, but total amounts of 24:0 and 24:1 species showed little
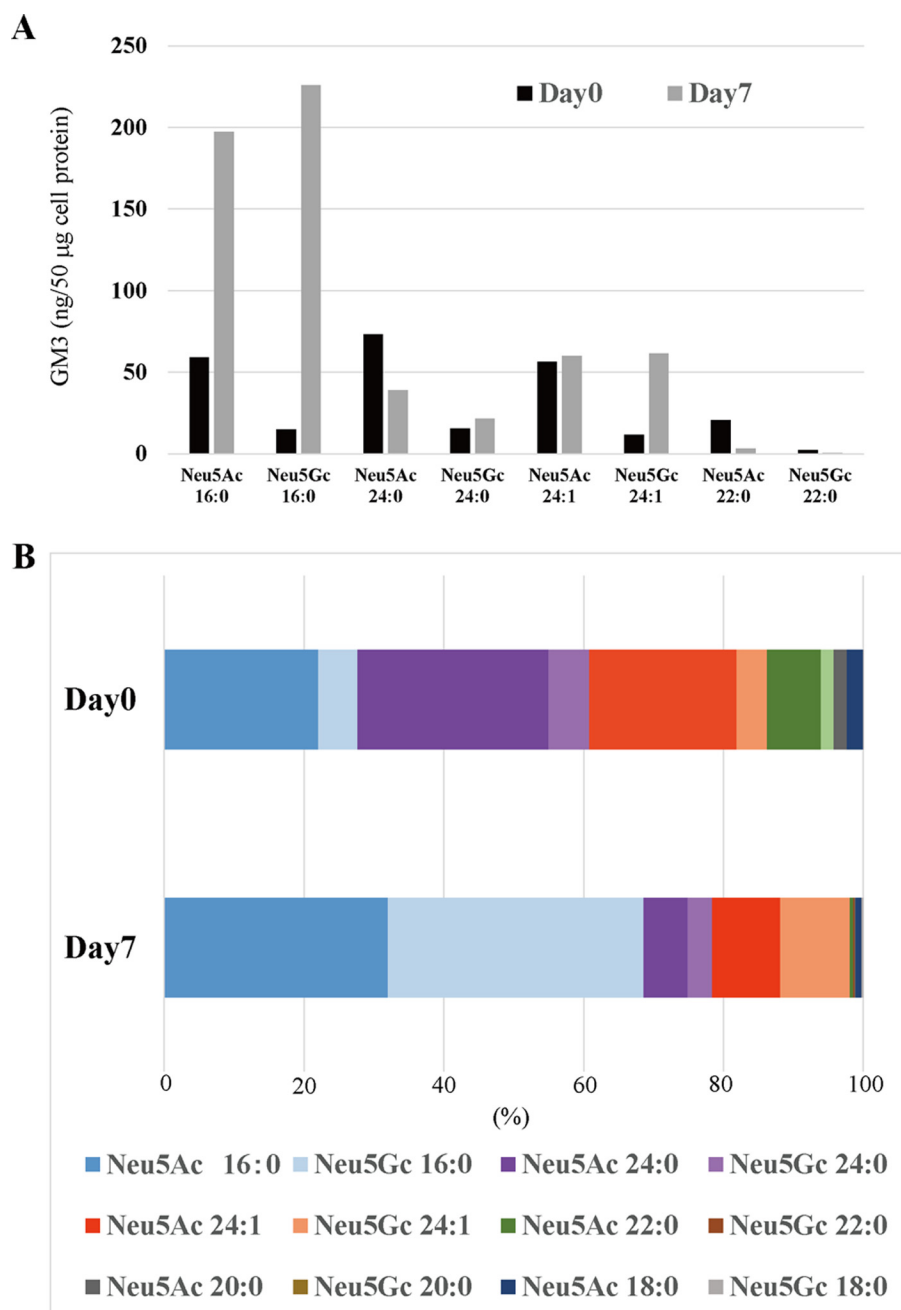
Figure 5. LC-MS/MS analysis of GM3 molecular species during C2C12 differentiation. *A*, levels of GM3 molecular species in C2C12 cells. The eight most abundant species on day 0 (*black bars*) and day 7 (*gray bars*) are shown. The amount of each species was quantified by LC-MS/MS using Neu5Ac GM3 (d18:1-[^{13}C]16:0) as the internal standard, as described under "Experimental procedures." *y* axis, amount of GM3 species (ng) present per 50 μg of cell protein. *B*, proportions of GM3 molecular species on days 0 and 7. Amounts of individual species were determined, and their proportions were calculated.

change (Fig. 5*A*). The proportion of 16:0 species increased markedly during differentiation (Fig. 5, *A* and *B*).

Expression of Cer synthases

Ceramide synthase (CerS) enzymes regulate synthesis of the various Cer species. Six types of mammalian CerS have been reported. Each CerS has a preference for a unique range of acyl-CoA groups and, therefore, controls a particular subset of Cer species. We used real-time PCR to determine expression levels of CerS1 through CerS6 in C2C12 cells. The predominant forms detected in these cells were CerS1, -2, -5, and -6. CerS2,

which catalyzes synthesis of ceramide with very long acyl chains such as C24, was most abundant in C2C12. CerS2 was slightly increased after the induction of differentiation, but it was decreased sharply during the differentiation process. On the other hand the levels of CerS5 and -6, which catalyze C16-Cer synthesis, remained constant (Fig. 6*A*). Therefore, the increase of GM3 C16 species after differentiation (Fig. 5) could be attributed to the marked decrease of CerS2 expression during the differentiation process (Fig. 6*A*).

We also examined changes in mRNA expression levels of fatty acyl-CoA elongases (Elovls) during differentiation. Levels

A

B
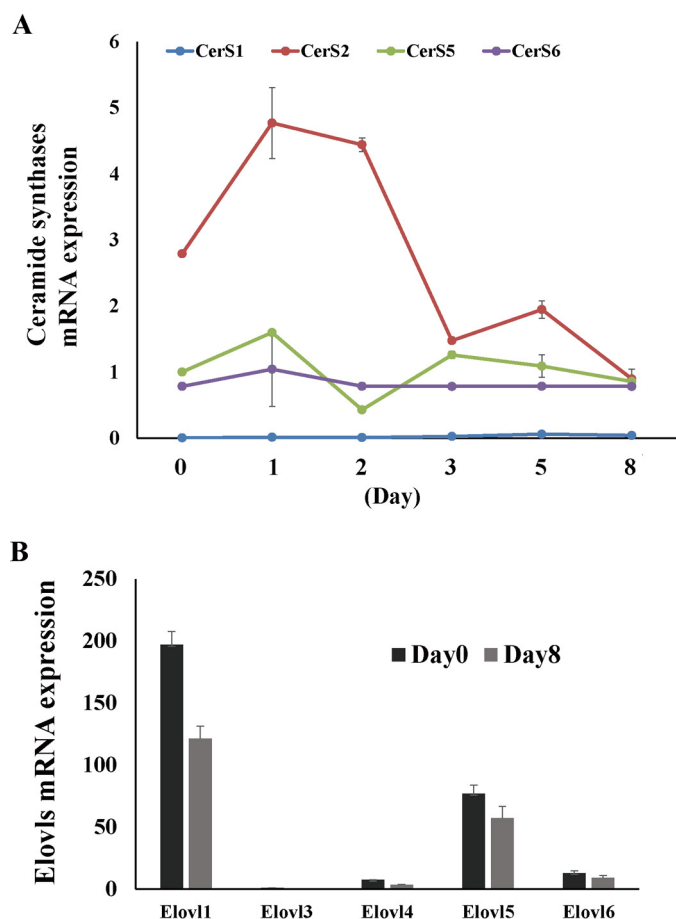
Figure 6. Changes in expression of Cer synthase mRNAs during C2C12 differentiation. *A*, expression levels of CerS mRNAs, determined by quantitative RT-PCR. -Fold change was calculated as $2^{-\Delta\Delta\pm CT}$ with tubulin used as the endogenous control. *B*, expression levels of Elovl mRNAs during differentiation, determined by quantitative RT-PCR. Data represent the relative gene expression in cells of each day compared with that in cells of day 0 (set to 1.0 separately for each target gene). Average -fold change obtained from three experiments is shown the means ± S.D.

of all five Elovls examined were lower on day 8 than on day 0 (Fig. 6*B*). This trend may also explain in part the increase of shorter acyl-chain Cer species.

Effects of exogenous sialic acid and GM3 species on cell morphology

Sialic acid and acyl chain structures of GM3 showed notable changes during C2C12 cell differentiation. The potential role of such changes was investigated by adding various sialic acid and GM3 molecular species to culture medium.

Sialic acid monosaccharide (Neu5Ac or Neu5Gc) was added during medium change each day to change the sialic acid species of sialylglycoconjugates. Treatment with 2 mM Neu5Ac or Neu5Gc efficiently increased intracellular Sia monosaccharide (Fig. 7*A*, *left panel*), so exogenous sialic acids were taken up by C2C12 cells. After 2 days the amount of lipid-linked Neu5Gc exceeded that of Neu5Ac in cells treated with 2 mM Neu5Gc, although Neu5Ac was the major sialic acid in normal and Neu5Ac-treated cells (Fig. 7*A*, *right panel*). Thus, we were able to change the ratio of sialic acid species in gangliosides by treatment with Neu5Gc. Cell morphology on day 6 is shown in Fig. 7, *B* and *C*.

Sialic acid species differentially affected morphology of myoblasts and/or myofibers. The ratio of long fibers was increased by treatment with Neu5Gc (Fig. 7*C*, *right panel*). And the formed fiber width was small (Fig. 7*C*, *left panel*). Therefore, cells treated with Neu5Gc monosaccharide formed longer, narrower myofibers. Neu5Ac or Neu5Gc treatment had no effect on the expression of differentiation marker proteins myogenin and MyHC (Fig. 7*D*, *left panel*). However, phosphorylation of paxillin, which regulates adhesion state, was increased by treatment with Neu5Gc (Fig. 7*D*, *right panel*). These findings suggest that sialic acid affects cell morphology via control of cytoskeleton formation or myofiber adhesion state.

Although Neu5Ac was taken up by cells during Neu5Ac treatment, the quality and quantity of glycosphingolipids was not drastically changed (Fig. 7*A*). The ratio of shorter length myotubes was slightly increased by Neu5Ac treatment. These changes may not be an effect of only change in GLSs, although these results suggest that extracellular sialic acid affected myoblast differentiation.

Exogenous gangliosides can be inserted into the outer leaflet of plasma membranes and be partially taken up and metabolized (26). We confirmed the uptake and increase of GM3 in cells by TLC and fluorometric HPLC (Fig. 8*A*). 25 μM exogenous GM3 efficiently increased cellular gangliosides (Fig. 8*A*, *left panel*) and lipid linked sialic acids (Fig. 8*A*, *right panel*). Therefore, we added GM3 species, shorter (16:0) species, which are the major species after differentiation, and longer (24:0 or 18:0) species, which are the major species before differentiation to evaluate their properties. In experiments with different GM3 molecular species, d18:1–16:0 species were well aligned and formed numerous myotubes, whereas cells treated with GM3 d18:1–18:0 or d18:1–24:0 species were poorly aligned and formed fewer myotubes (Fig. 8*B*); the ratio of cells with shorter length and larger width was increased when treated with GM3 d18:1–18:0 or d18:1–24:0 species (Fig. 8*C*). Although expression level of myogenin was relatively unaffected by treatment with different GM3 molecular species, the level of MyHC was notably reduced by treatment with GM3 d18:1–18:0 or d18:1–24:0 species (Fig. 8*D*). Cells treated with GM3 d18:1–16:0 formed relatively longer myofibers.

These findings indicate that increased longer acyl-chain GM3 species inhibit some signaling in differentiation processes such as fusion process and/or formation of myotubes, whereas shorter acyl-chain GM3 species do not inhibit, or might, enhance.

In this study we found an association of GM3 lipid species change and differentiation in myoblast. The results shown in Fig. 7 and in Fig. 8 are consistent with the hypothesis that myoblasts may regulate their differentiation by changing GSLs species.

Discussion

Skeletal muscle differentiation comprises a chain of complex processes in which cell plasma membranes play a crucial role. Cell-to-cell adhesion and recognition are essential for the differentiation process. It is necessary for progenitor cells to contact numerous similar cells and respond to inductive signals in order to undergo a coordinated process of differentiation. In
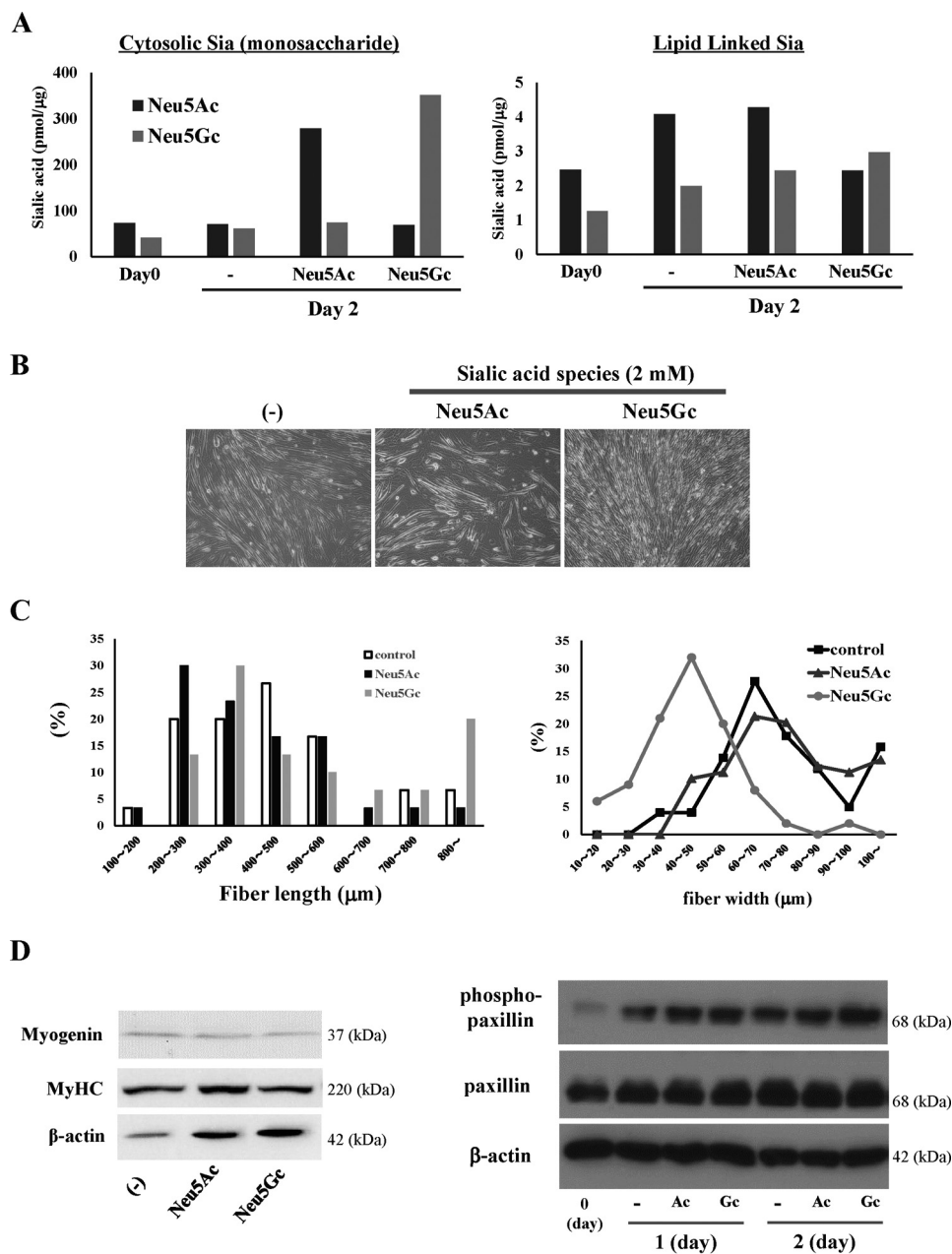
Figure 7. Effects of sialic acid monosaccharide supplementation on C2C12 differentiation. *A*, uptake and utilization of exogenous sialic acids in C2C12 cells. 2 mM Neu5Ac or Neu5Gc was added to the differentiation medium. After 2 days Sia monosaccharide in cytosol (*left panel*) and lipid-bound Sia (*right panel*) were measured as described under "Experimental procedures." *B*, phase-contrast microphotographs on day 6 of cells treated with sialic acid (2 mM) in DM. *C*, effects of exogenous sialic acids on morphology of myofibers. The ratio of each fiber length (*right panel*) and width (*left panel*) are shown (control and Neu5Gc; *n* = 100, Neu5Ac; *n* = 89). *D*, expression levels, on day 6 of differentiation, of marker proteins myogenin and MyHC in cells treated with sialic acid in DM (*right panel*). Shown are the effects of sialic acids on the phosphorylation state of paxillin on days 1 and 2 (*left panel*). Shown are representative Western blot images.

the final steps of differentiation, plasma membranes fuse with each other (14, 15, 27). Biochemical characteristics of plasma membranes thus have important effects on skeletal muscle differentiation. GSLs, particularly gangliosides, help determine plasma membrane properties and play essential roles in regulating many biological processes, including cell-cell interactions and signal transduction (1, 2). Expression of GM3, GM2, GM1, and GD1a has been reported in myoblast cell line C2C12 (16–18); however, changes in ganglioside expression and functions of specific ganglioside species during myogenic differentiation have not been studied. We analyzed changes in gangli-

oside species during myogenic differentiation using C2C12 cells as a model. We demonstrated for the first time striking changes in quantity and quality of gangliosides during the differentiation process. Alterations of molecular species of GM3, the major ganglioside in C2C12 cells, were particularly notable. Sialic acid species in GM3 were changed from Neu5Ac to Neu5Gc through elevated expression of hydroxylase CMAH. GM3 species with 16:0 acyl chains were greatly increased. To elucidate the function of this GM3 molecular species change, we added sialic acid monosaccharide or synthetic GM3 acyl chain species to culture medium. Our findings (Figs. 6 and 7)
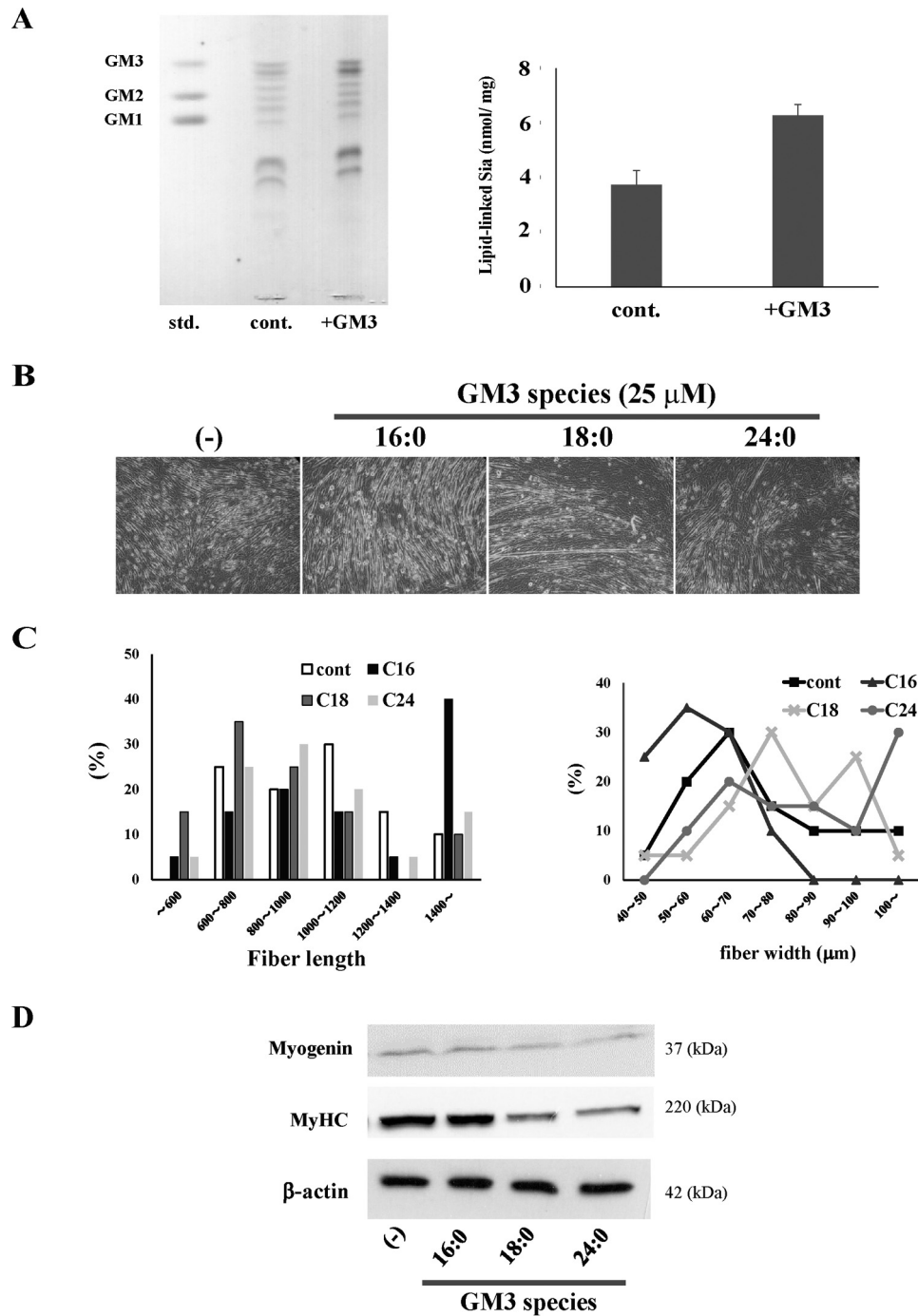
Figure 8. Effects of GM3 acyl chain structure on C2C12 differentiation. *A*, uptake of exogenous GM3. Shown is TLC analysis (*right panel*), and the amounts of lipid-linked sialic acids (*left panel*) of C2C12 cells treated with 25 mM GM3 for 24 h. *B*, phase-contrast microphotographs on day 6 of cells treated with three GM3 species (25 μM). *C*, effects of exogenous sialic acids on morphology of myofibers. The ratio of each fiber length (*right panel*) and width (*left panel*) are shown (*n* = 20). *D*, expression levels on day 6 of differentiation marker proteins myogenin and MyHC in cells treated with three GM3 species. Shown are representative Western blot images.

indicate that sialic acid species affect cell morphology and that GM3 acyl chain structures play key roles in regulating differentiation.

In regard to GM3 function in myogenic differentiation, previous studies indicate that sialidase (Neu3), which is localized in the plasma membrane and hydrolyzes GM3 and other gangliosides, affects differentiation of C2C12 cells. Neu3 overexpression delayed myoblast differentiation and induced hypertrophic myotube formation, whereas differentiation was inhibited by Neu3 gene silencing (16–18). The Neu3 protein *per se* presumably modulates certain cell functions, but these studies suggest that GM3 in appropriate amounts also plays an important role in normal C2C12 differentiation, most likely via modulation of EGFR signaling. We used a GSL synthesis inhibitor to confirm that GSLs in appropriate amounts are important in myofiber formation (data not shown). Thus, proper amounts of GM3 are required at each step in the process for normal myogenic differentiation. We observed here for the first time

striking changes in GM3 quality during differentiation; *i.e.* major alterations in sialic acid species and acyl chain structures (Figs. 2–4). Our findings suggest that ganglioside quality as well as quantity is important at each step for normal myogenic differentiation.

Sialic acid species and the acyl chain structures of gangliosides are involved in maintaining cell membrane properties and lipid microdomain structures. Hashimoto and co-workers (28, 29) observed that disruption of lipid rafts by cholesterol depletion directly blocked the plasma membrane fusion that normally occurs as part of myogenic cell fusion. The molecular mechanisms that control cell fusion and other steps of myogenic differentiation remain to be elucidated; however, plasma membrane rafts clearly play an important role. A number of membrane molecules have been implicated in regulation of myogenic differentiation. Extracellular matrix receptor integrins (30) and adhesion molecules such as cadherins, NCAM, and CD9 (31–33) are involved in regulation of the recognition and adhesion steps in myoblast differentiation and maintenance of myofibers. Crucial molecules (*e.g.* BAI1, myomaker) involved in regulation of initiation signals for myogenic differentiation and plasma membrane fusion were discovered in 2013 (34, 35). Such transmembrane proteins are localized in specific regions of the plasma membrane during differentiation; it is thus possible that various GM3 molecular species interact specifically with the proteins, directly or indirectly, to regulate their functions and localization. Membrane fluidity affects myogenic differentiation, particularly the plasma membrane fusion process (36–38); thus, another possibility is that concentrations of various GSL molecular species in myoblasts help regulate membrane fluidity and are strictly controlled for this purpose.

Our knowledge of molecular mechanisms that regulate distribution and expression of GSL molecular species and other plasma membrane molecules remains fragmentary. The CerS enzymes provide one regulatory mechanism for expression of GSL acyl chain molecular species. Six mammalian CerSs have been described, each utilizing fatty acyl CoAs with differing chain lengths for *N*-acylation of the sphingoid long chain base. CerS5 and CerS6 catalyze synthesis of C16 acyl chain Cer species (9, 10). Most studies to date focused on roles of CerSs in regulation of sphingolipids have relied on CerS overexpression to increase Cer synthesis. Therefore, it remains unclear how individual CerSs contribute to a steady-state sphingolipid pool in mammalian cells, and whether maintenance of sphingolipids with specific acyl chains depends on specific CerSs (39). C16 GSL species were strikingly increased during C2C12 differentiation in the present study (Fig. 5). The increase of GM3 C16 species after differentiation could be attributed to the marked decrease of CerS2 expression during the process of differentiation (Fig. 6*A*). We also observed that expression levels of Elovls declined during myogenic differentiation, which may help account for increased levels of shorter acyl-chain species (Fig. 6*B*). Future studies may reveal unknown mechanisms for regulation of GSL molecular species by inter-regulation of CerSs and Elovls.

By treatment with exogenous GM3 species, cellular gangliosides were changed (Fig. 8). We found that increased longer acyl-chain GM3 species inhibited differentiation, whereas shorter acyl-chain GM3 did not result in inhibition (Fig. 8, *B* and *C*). These results suggest that myoblasts regulate some signaling processes during differentiation, such as fusion processes and/or formation of myotubes, by changing the metabolism of ganglioside acyl chain species.

Besides changes in acyl chains of GM3 molecular species, the present study demonstrates for the first time changes of sialic acid species from Neu5Ac to Neu5Gc during differentiation. We also observed morphological changes in myotubes after treatment with Neu5Gc (Fig. 7, *B* and *C*). This phenomenon suggests a function for Neu5Gc glycoconjugates in the process of myogenic differentiation, especially in the regulation of cell morphology. Although during the exogenous treatment we employed, the ratio of Neu5Gc was increased in both glycoproteins and glycolipids (data not shown); therefore, we cannot concluded the effects observed were the result of Neu5Gc GM3 alone. Several groups have described changes of sialic acid species on glycans during various biological processes (40–43). It appears that Neu5Gc expression can also be affected by cell activation and disease status. *Cmah* mRNA expression is altered during lymphocyte activation in mice (41, 42), and Neu5Gc treatment modifies interactions between glycans and their binding proteins. Taken together, these past and present findings indicate that the change of sialic acid species from Neu5Ac to Neu5Gc is crucial for myogenic differentiation in mice. Deletion of *Cmah* in mice increased the severity of muscular dystrophy (44, 45), suggesting that this gene is a genetic modifier of muscle homeostasis. Taken together, our results suggest that myoblasts regulate their differentiation by changing the metabolism of sialic acids, ceramide, and, consequently, gangliosides.

We want to elucidate the function of specific GM3 molecular species, which have their expression levels affected before and after myogenic differentiation, especially focusing on NeuGc GM3 with a C16 acyl chain as shown in Fig. 5*A*. We confirmed the change in expression of some genes related to the synthesis of this molecule. Therefore, we tried to modify the expression of these genes (such as GM3 synthase, *Cmah*, and CerSs) to show their function in myogenic differentiation. However, we could not establish gene-modified C2C12 cells while maintaining differentiation potency. Therefore, we will report further on these investigations in our next manuscript.

In conclusion, the present results demonstrate that quantity and quality of GM3 change greatly during myoblast C2C12 differentiation and suggest that these changes play a key role in regulation of the differentiation process. These findings help clarify the significance of GSL structural diversity in mammalian cells. Our ongoing studies, using genetically modified mice and cells, are focused on roles of GM3 molecular species in function and regeneration of muscle cells and tissues.

Experimental procedures

Materials

Hybridoma cells producing anti-GM3 (Neu5Gc) monoclonal antibody (mAb) GMR8 were kindly donated by Ikuo Kawashima (20), RIKEN BioResource Center. Anti-GM3 (Neu5Ac) mAb

GMR6 was from Seikagaku Co. (Tokyo, Japan). Anti-myogenin and myosin heavy chain antibodies were from e-Bioscience (Santa Clara, CA). GM3 molecular species were synthesized according to previous reports (46, 47). Neu5Ac GM3 (d18:1-[^{13}C]16:0), an internal standard for quantification by LC-MS/MS, was from Tokyo Chemical Industry (Tokyo, Japan).

Cell culture

C2C12 myoblast cells were obtained from RIKEN Bio-Resource Center (Tsukuba, Japan) and cultured in Dulbecco's modified Eagle's medium (DMEM; Nacalai; Kyoto, Japan) containing 10% heat-inactivated fetal bovine serum at 37 °C in 5% CO_2 atmosphere. To induce differentiation, growth medium was replaced with DMEM containing 2% horse serum (DM) when cells reached ~90% confluency. Cells were replenished with fresh DM every 24 h. To evaluate the effects of exogenous sialic acids, Neu5Ac or Neu5Gc (2 mM) were added to DM. To evaluate the effects of exogenous GM3, synthetic GM3 acyl chain species (25 μM) were added to DM.

Analysis of GSLs

Analysis of GSLs by TLC was performed as described originally in Refs. 48 and 49 and slightly modified (50). In brief, total cell lipids were extracted using chloroform/methanol, and extracts were applied to DEAE-Sephadex A-25 column equilibrated with chloroform/methanol/water (30:60:8, v/v/v). The column was washed with the same solvent, and acidic GSL fraction was eluted with chloroform/methanol/1 M sodium acetate (30:60:8, v/v/v). Acidic and neutral lipids were subjected to mild alkaline hydrolysis and desalted using a Sep-Pak C18 cartridge. Acidic GSLs were spotted on a TLC plate and developed with chloroform/methanol/0.2% $CaCl_2$ (60:25:4, v/v/v). GSLs were visualized by orcinol/sulfuric acid staining.

TLC immunostaining

Acidic GSLs were spotted on a TLC plate and developed with chloroform/methanol/0.2% $CaCl_2$ (60:25:4, v/v/v). The dried plate was dipped in cyclohexane containing 0.1% (w/v) poly-(isobutyl methacrylate) for 1 min, blocked by incubation in PBS containing 1% BSA at room temperature for 1 h, incubated with anti-GM3 mAb GMR6 (GM3(Neu5Ac) specific) or GMR8 (GM3(Neu5Gc) specific) in PBS containing 1% BSA at room temperature for 2 h, washed 5 times with PBS, and incubated with anti-mouse IgM horseradish peroxidase (HRP)-conjugated antibody at 37 °C for 1 h. HRP was detected by the addition of appropriate substrates following the manufacturer's instructions.

Sialic acid analysis by fluorometric HPLC

Sialic acids were hydrolyzed from acidic GSL fractions by trifluoroacetic acid. An aliquot of the supernatant was lyophilized and then incubated with 1,2-diamino-4,5-methylene dioxybenzene as described previously (51). 1,2-Diamino-4,5-methylene dioxybenzene-labeled sialic acids were separated and detected using an HPLC system (JASCO; Tokyo, Japan) equipped with a reversed-phase C18 column (Wakopak Handy-ODS (4.6 mm × 250 mm); Wako Pure Chemical, Osaka, Japan).

Table 1
Primers used to specifically enhance each mRNA fragment

Gene		Primer sequence
CerS1	Forward	5′–TGACTGGTCAGATGCGTGA–3′
	Reverse	5′–TCAGTGGCTTCTCGGCTTT–3′
CerS2	Forward	5′–TCATCATCACTCGGCTGGT–3′
	Reverse	5′–AGCCAA AGAAGGCAGGGTA–3′
CerS3	Forward	5′–ATCTCGAGCCCTTCTTCTCC–3′
	Reverse	5′–CTGGACGTTCTGCGTGAAT–3′
CerS4	Forward	5′–TGCGCATGCTCTACAGTTTC–3′
	Reverse	5′–CTCGAGCCATCCCATTCTT–3′
CerS5	Forward	5′–TCCATGCCATCTGGTCCTA–3′
	Reverse	5′–TGCTGCCAGAGAGGTTGTT–3′
CerS6	Forward	5′–GGGTTGAACTGCTTCTGGTC–3′
	Reverse	5′–TTTCTTCCCTGGAGGCTCT–3′
Cmah	Forward	5′–GAAAGGCCTGTGTTTTGGAA–3′
	Reverse	5′–TCATGAACCGCAGACTTTTG–3′
St3gal5	Forward	5′–GTGGACCCTGACCGGATAAAG–3′
(GM3 S)	Reverse	5′–AACAGAGCCATAGCCGTCTTC–3′
Tubulin	Forward	5′–CACTACACCATTGGCAAGGA–3′
	Reverse	5′–TGTGGAAAACCAAGAAGCCC–3′
Elovl 1	Forward	5′–GGTGGGGGATAAAAATTGCT–3′
	Reverse	5′–CCAAGGGCAGACAATCCATA–3′
Elovl 2	Forward	5′–GACGCTGGTCATCCTGTTCT–3′
	Reverse	5′–GCTTTGGGGAAACCATTCTT–3′
Elovl 3	Forward	5′–TTTGCCATCTACACGGATGA–3′
	Reverse	5′–CGTGTCTCCCAGTTCAACAA–3′
Elovl 4	Forward	5′–TTTGGTGGAAGCGATACCTG–3′
	Reverse	5′–ATGTCCGAGTGTAGAAGTTG–3′
Elovl 5	Forward	5′–CTCTCGGGTGGCTGTTTTT–3′
	Reverse	5′–AGAGGCCCCTTTCTTGTTGT–3′
Elovl 6	Forward	5′–ACAATGGACCTGTCAGCAAA–3′
	Reverse	5′–GTACCAGTGCAGGAAGATCAGT–3′
Elovl 7	Forward	5′–ATGGGACCAGCCTACCAGAA–3′
	Reverse	5′–TTGCAGTCCTCCATGAAGAA–3′

RT-PCR

Total RNAs were prepared from cells using TRIzol reagent. Reverse transcription of total RNA was performed to generate first-strand cDNA. For detection of cDNA of mouse CMP-sialic acid hydroxylase, we performed RT-PCR assays using a primer set based on sequences of CMP-sialic acid hydroxylase (5′-ctgatcccaggtctcctgaa-3′, 5′-agcctctccaaccagtcaga-3′) and GAPDH (5′-acaaaatggtgaaggtcggt-3′, 5′-tccagggtttcttactcctt-3′). For quantitative real-time PCR, cDNA was prepared from total RNA using a PrimeScript™ RT Reagent kit (Takara Bio). RT-PCR was performed and analyzed using SsoFast™ EvaGreen Supermix on a Real-Time PCR system (Bio-Rad). Expression values were normalized to tubulin, and relative mRNA expression was calculated as described by Livak and Schmittgen (52). Primers used are listed in Table 1.

Mass spectrometric analysis

Neu5Ac GM3 (d18:1-[^{13}C]16:0) was added to acidic GSL samples as the internal standard. GM3 molecular species were quantified using HPLC coupled with electrospray ionization tandem mass spectrometry (MS/MS) in multiple reaction-monitoring negative ionization mode. The triple-stage quadrupole (TSQ) Vantage AM instrument (Thermo Fisher, Waltham, MA) was calibrated by directly infusing a mixture of GM3 species extracted from milk, and all ion source parameters and ionization conditions were optimized to improve sensitivity. GSLs were dissolved in methanol, injected onto an HPLC pump (Accela 1250, Thermo Fisher), and separated using a Develosil carbon 30 column (C30-UG-3–1 × 50 mm, Nomura Co.; Aichi, Japan). The gradient program started with 100% solvent A (20% H_2O, 50% 2-propanol, 30% methanol con-

Table 2

Mass spectrometer settings and MRM transition pairs

Q, quadrupole; CE, collision energy; S-lens, stacked-ring ion guide; RF, radio frequency.

Molecular species (Sia)	Molecular species (Cer)	Q1	Q3	CE	S-lens RF amplitude
		m/z	*m/z*	*eV*	
GM3 (Neu5Ac) [M-H]⁻					
	d18:1–16:1	1149.7	289.9	53	276
	d18:1–16:0	1151.7	289.9	53	276
	d18:1-h16:1	1165.7	289.9	53	276
	d18:1-[¹³C]16:0	1167.9	289.9	53	276
	d18:1–18:1	1177.7	289.9	53	276
	d18:1–18:0	1179.7	289.9	53	276
	d18:1-h18:1	1193.7	289.9	53	276
	d18:1-h18:0	1195.7	289.9	53	276
	d18:1–20:1	1205.7	289.9	53	276
	d18:1–20:0	1207.7	289.9	53	276
	d18:1–21:1	1219.7	289.9	53	276
	d18:1–21:0	1221.7	289.9	53	276
	d18:1-h20:0	1223.7	289.9	53	276
	d18:1–22:1	1233.7	289.9	53	276
	d18:1–22:0	1235.7	289.9	53	276
	d18:1-h21:0	1237.7	289.9	53	276
	d18:1–23:1	1247.7	289.9	53	276
	d18:1–23:0	1249.7	289.9	53	276
	d18:1-h22:0	1251.7	289.9	53	276
	d18:1–24:1	1261.8	289.9	53	276
	d18:1–24:0	1263.8	289.9	53	276
	d18:1-h23:0	1265.8	289.9	53	276
	d18:1-h24:1	1277.8	289.9	53	276
	d18:1-h24:0	1279.8	289.9	53	276
	d18:1–16:1	1165.7	305.9	53	276
GM3 (Neu5Gc) [M-H]⁻					
	d18:1–16:0	1167.7	305.9	53	276
	d18:1-h16:1	1181.7	305.9	53	276
	d18:1–18:1	1193.7	305.9	53	276
	d18:1–18:0	1195.7	305.9	53	276
	d18:1-h18:1	1209.7	305.9	53	276
	d18:1-h18:0	1211.7	305.9	53	276
	d18:1–20:1	1221.7	305.9	53	276
	d18:1–20:0	1223.7	305.9	53	276
	d18:1–21:1	1235.7	305.9	53	276
	d18:1–21:0	1237.7	305.9	53	276
	d18:1-h20:0	1239.7	305.9	53	276
	d18:1–22:1	1249.7	305.9	53	276
	d18:1–22:0	1251.7	305.9	53	276
	d18:1-h21:0	1253.7	305.9	53	276
	d18:1–23:1	1263.7	305.9	53	276
	d18:1–23:0	1265.7	305.9	53	276
	d18:1-h22:0	1267.7	305.9	53	276
	d18:1–24:1	1277.8	305.9	53	276
	d18:1–24:0	1279.8	305.9	53	276
	d18:1-h23:0	1281.8	305.9	53	276
	d18:1-h24:1	1293.8	305.9	53	276
	d18:1-h24:0	1295.8	305.9	53	276

taining 0.1% acetic acid and 0.1% ammonia) for 5 min, then ramped to 100% solvent B (2% H$_2$O, 50% 2-propanol, 48% methanol containing 0.1% acetic acid, and 0.1% ammonia) over 30 min. 100% solvent B was maintained for 4 min, then the solvent was returned to 100% solvent A over 1 min and held there for 10 min. Flow was 50 μl/min throughout the chromatographic run. −2500 V potential was applied between ion source and electrospray needle. The carrier gas was nitrogen. Relative abundances of molecular species were assessed based on relative percentage of internal standard. All GM3 molecular species may not necessarily have identical ionization efficiencies; however, because of limited availability of pure molecular species standards, we assumed that all species have ionization efficiencies comparable with that of the internal standard. Thus, in evaluating relative abundances of molecular species, detected amounts are compared that may not necessarily rep-

resent absolute amounts (13). The details for the assignment of ganglioside molecular species are shown in Table 2.

References

1. Jennemann, R., and Gröne, H. J. (2013) Cell-specific *in vivo* functions of glycosphingolipids: lessons from genetic deletions of enzymes involved in glycosphingolipid synthesis. *Prog. Lipid Res.* **52,** 231–248
2. Regina Todeschini, A., and Hakomori, S. I. (2008) Functional role of glycosphingolipids and gangliosides in control of cell adhesion, motility, and growth, through glycosynaptic microdomains. *Biochim. Biophys. Acta* **1780,** 421–433
3. Schnaar, R. L., Gerardy-Schahn, R., and Hildebrandt, H. (2014) Sialic acids in the brain: gangliosides and polysialic acid in nervous system development, stability, disease, and regeneration. *Physiol. Rev.* **94,** 461–518
4. Inokuchi, J. (2010) Membrane microdomains and insulin resistance. *FEBS Lett.* **584,** 1864–1871
5. Inokuchi, J. (2011) Physiopathological function of hematoside (GM3 ganglioside). *Proc. Jpn. Acad. Ser. B. Phys. Biol. Sci.* **87,** 179–198
6. Inokuchi, J. (2014) GM3 and diabetes. *Glycoconj. J.* **31,** 193–197
7. Kabayama, K., Sato, T., Kitamura, F., Uemura, S., Kang, B. W., Igarashi, Y., and Inokuchi, J. (2005) TNFα-induced insulin resistance in adipocytes as a membrane microdomain disorder: involvement of ganglioside GM3. *Glycobiology* **15,** 21–29
8. Kabayama, K., Sato, T., Saito, K., Loberto, N., Prinetti, A., Sonnino, S., Kinjo, M., Igarashi, Y., and Inokuchi, J. (2007) Dissociation of the insulin receptor and caveolin-1 complex by ganglioside GM3 in the state of insulin resistance. *Proc. Natl. Acad. Sci. U.S.A.* **104,** 13678–13683
9. Mullen, T. D., Hannun, Y. A., and Obeid, L. M. (2012) Ceramide synthases at the centre of sphingolipid metabolism and biology. *Biochem. J.* **441,** 789–802
10. Park, J. W., Park, W. J., and Futerman, A. H. (2014) Ceramide synthases as potential targets for therapeutic intervention in human diseases. *Biochim. Biophys. Acta* **1841,** 671–681
11. Angata, T., and Varki, A. (2002) Chemical diversity in the sialic acids and related α-keto acids: an evolutionary perspective. *Chem. Rev.* **102,** 439–469
12. Hayashi, N., Chiba, H., Kuronuma, K., Go, S., Hasegawa, Y., Takahashi, M., Gasa, S., Watanabe, A., Hasegawa, T., Kuroki, Y., Inokuchi, J., and Takahashi, H. (2013) Detection of N-glycolyated gangliosides in non-small-cell lung cancer using GMR8 monoclonal antibody. *Cancer Sci.* **104,** 43–47
13. Veillon, L., Go, S., Matsuyama, W., Suzuki, A., Nagasaki, M., Yatomi, Y., and Inokuchi, J. (2015) Identification of ganglioside GM3 molecular species in human serum associated with risk factors of metabolic syndrome. *PloS ONE* **10,** e0129645
14. Hindi, S. M., Tajrishi, M. M., and Kumar, A. (2013) Signaling mechanisms in mammalian myoblast fusion. *Sci. Signal.* **6,** re2
15. Krauss, R. S., Cole, F., Gaio, U., Takaesu, G., Zhang, W., and Kang, J. S. (2005) Close encounters: regulation of vertebrate skeletal myogenesis by cell-cell contact. *J. Cell Sci.* **118,** 2355–2362
16. Anastasia, L., Papini, N., Colazzo, F., Palazzolo, G., Tringali, C., Dileo, L., Piccoli, M., Conforti, E., Sitzia, C., Monti, E., Sampaolesi, M., Tettamanti, G., and Venerando, B. (2008) NEU3 sialidase strictly modulates GM3 levels in skeletal myoblasts C2C12 thus favoring their differentiation and protecting them from apoptosis. *J. Biol. Chem.* **283,** 36265–36271

17. Papini, N., Anastasia, L., Tringali, C., Dileo, L., Carubelli, I., Sampaolesi, M., Monti, E., Tettamanti, G., and Venerando, B. (2012) MmNEU3 sialidase over-expression in C2C12 myoblasts delays differentiation and induces hypertrophic myotube formation. *J. Cell. Biochem.* **113,** 2967–2978

18. Scaringi, R., Piccoli, M., Papini, N., Cirillo, F., Conforti, E., Bergante, S., Tringali, C., Garatti, A., Gelfi, C., Venerando, B., Menicanti, L., Tettamanti, G., and Anastasia, L. (2013) NEU3 sialidase is activated under hypoxia and protects skeletal muscle cells from apoptosis through the activation of the epidermal growth factor receptor signaling pathway and the hypoxia-inducible factor (HIF)-1α. *J. Biol. Chem.* **288,** 3153–3162

19. Singhal, N., and Martin, P. T. (2015) A role for Galgt1 in skeletal muscle regeneration. *Skelet. Muscle* **5,** 3

20. Ozawa, H., Kawashima, I., and Tai, T. (1992) Generation of murine monoclonal antibodies specific for *N*-glycolylneuraminic acid-containing gangliosides. *Arch. Biochem. Biophys.* **294,** 427–433

21. Samraj, A. N., Pearce, O. M., Läubli, H., Crittenden, A. N., Bergfeld, A. K., Banda, K., Gregg, C. J., Bingman, A. E., Secrest, P., Diaz, S. L., Varki, N. M., and Varki, A. (2015) A red meat-derived glycan promotes inflammation and cancer progression. *Proc. Natl. Acad. Sci. U.S.A.* **112,** 542–547

22. Varki, A. (2001) *N*-glycolylneuraminic acid deficiency in humans. *Biochimie* **83,** 615–622

23. Yin, J., Hashimoto, A., Izawa, M., Miyazaki, K., Chen, G. Y., Takematsu, H., Kozutsumi, Y., Suzuki, A., Furuhata, K., Cheng, F. L., Lin, C. H., Sato, C., Kitajima, K., and Kannagi, R. (2006) Hypoxic culture induces expression of sialin, a sialic acid transporter, and cancer-associated gangliosides containing non-human sialic acid on human cancer cells. *Cancer Res.* **66,** 2937–2945

24. Kawano, T., Koyama, S., Takematsu, H., Kozutsumi, Y., Kawasaki, H., Kawashima, S., Kawasaki, T., and Suzuki, A. (1995) Molecular cloning of cytidine monophospho-*N*-acetylneuraminic acid hydroxylase: regulation of species- and tissue-specific expression of *N*-glycolylneuraminic acid. *J. Biol. Chem.* **270,** 16458–16463

25. Schlenzka, W., Shaw, L., Kelm, S., Schmidt, C. L., Bill, E., Trautwein, A. X., Lottspeich, F., and Schauer, R. (1996) CMP-N-acetylneuraminic acid hydroxylase: the first cytosolic Rieske iron-sulphur protein to be described in Eukarya. *FEBS Lett.* **385,** 197–200

26. Schwarzmann, G. (2001) Uptake and metabolism of exogenous glycosphingolipids by cultured cells. *Semin. Cell Dev. Biol.* **12,** 163–171

27. Horsley, V., and Pavlath, G. K. (2004) Forming a multinucleated cell: molecules that regulate myoblast fusion. *Cells Tissues Organs* **176,** 67–78

28. Mukai, A., Kurisaki, T., Sato, S. B., Kobayashi, T., Kondoh, G., and Hashimoto, N. (2009) Dynamic clustering and dispersion of lipid rafts contribute to fusion competence of myogenic cells. *Exp. Cell Res.* **315,** 3052–3063

29. Mukai, A., and Hashimoto, N. (2008) Localized cyclic AMP-dependent protein kinase activity is required for myogenic cell fusion. *Exp. Cell Res.* **314,** 387–397

30. Schwander, M., Leu, M., Stumm, M., Dorchies, O. M., Ruegg, U. T., Schittny, J., and Müller, U. (2003) β1 integrins regulate myoblast fusion and sarcomere assembly. *Dev. Cell* **4,** 673–685

31. Charrin, S., Latil, M., Soave, S., Polesskaya, A., Chrétien, F., Boucheix, C., and Rubinstein, E. (2013) Normal muscle regeneration requires tight control of muscle cell fusion by tetraspanins CD9 and CD81. *Nat. Commun.* **4,** 1674

32. Ong, E., Suzuki, M., Belot, F., Yeh, J. C., Franceschini, I., Angata, K., Hindsgaul, O., and Fukuda, M. (2002) Biosynthesis of HNK-1 glycans on *O*-linked oligosaccharides attached to the neural cell adhesion molecule (NCAM): the requirement for core 2-β-1,6-*N*-acetylglucosaminyltransferase and the muscle-specific domain in NCAM. *J. Biol. Chem.* **277,** 18182–18190

33. Suzuki, M., Angata, K., Nakayama, J., and Fukuda, M. (2003) Polysialic acid and mucin type *O*-glycans on the neural cell adhesion molecule differentially regulate myoblast fusion. *J. Biol. Chem.* **278,** 49459–49468

34. Hochreiter-Hufford, A. E., Lee, C. S., Kinchen, J. M., Sokolowski, J. D., Arandjelovic, S., Call, J. A., Klibanov, A. L., Yan, Z., Mandell, J. W., and Ravichandran, K. S. (2013) Phosphatidylserine receptor BAI1 and apoptotic cells as new promoters of myoblast fusion. *Nature* **497,** 263–267

35. Millay, D. P., O'Rourke, J. R., Sutherland, L. B., Bezprozvannaya, S., Shelton, J. M., Bassel-Duby, R., and Olson, E. N. (2013) Myomaker is a membrane activator of myoblast fusion and muscle formation. *Nature* **499,** 301–305

36. Cornell, R. B., Nissley, S. M., and Horwitz, A. F. (1980) Cholesterol availability modulates myoblast fusion. *J. Cell Biol.* **86,** 820–824

37. Mermelstein, C. S., Portilho, D. M., Medeiros, R. B., Matos, A. R., Einicker-Lamas, M., Tortelote, G. G., Vieyra, A., and Costa, M. L. (2005) Cholesterol depletion by methyl-β-cyclodextrin enhances myoblast fusion and induces the formation of myotubes with disorganized nuclei. *Cell Tissue Res.* **319,** 289–297

38. Sekiya, T., Takenawa, T., and Nozawa, Y. (1984) Reorganization of membrane cholesterol during membrane fusion in myogenesis *in vitro*: a study using the filipin-cholesterol complex. *Cell Struct. Funct.* **9,** 143–155

39. Mullen, T. D., Spassieva, S., Jenkins, R. W., Kitatani, K., Bielawski, J., Hannun, Y. A., and Obeid, L. M. (2011) Selective knockdown of ceramide synthases reveals complex interregulation of sphingolipid metabolism. *J. Lipid Res.* **52,** 68–77

40. Casadesús, A. V., Fernández-Marrero, Y., Clavell, M., Gómez, J. A., Hernández, T., Moreno, E., and López-Requena, A. (2013) A shift from *N*-glycolyl- to *N*-acetylsialic acid in the GM3 ganglioside impairs tumor development in mouse lymphocytic leukemia cells. *Glycoconj. J.* **30,** 687–699

41. Naito, Y., Takematsu, H., Koyama, S., Miyake, S., Yamamoto, H., Fujinawa, R., Sugai, M., Okuno, Y., Tsujimoto, G., Yamaji, T., Hashimoto, Y., Itohara, S., Kawasaki, T., Suzuki, A., and Kozutsumi, Y. (2007) Germinal center marker GL7 probes activation-dependent repression of *N*-glycolylneuraminic acid, a sialic acid species involved in the negative modulation of B-cell activation. *Mol. Cell. Biol.* **27,** 3008–3022

42. Naito-Matsui, Y., Takada, S., Kano, Y., Iyoda, T., Sugai, M., Shimizu, A., Inaba, K., Nitschke, L., Tsubata, T., Oka, S., Kozutsumi, Y., and Takematsu, H. (2014) Functional evaluation of activation-dependent alterations in the sialoglycan composition of T cells. *J. Biol. Chem.* **289,** 1564–1579

43. Samraj, A. N., Läubli, H., Varki, N., and Varki, A. (2014) Involvement of a non-human sialic acid in human cancer. *Front. Oncol.* **4,** 33

44. Chandrasekharan, K., Yoon, J. H., Xu, Y., deVries, S., Camboni, M., Janssen, P. M., Varki, A., and Martin, P. T. (2010) A human-specific deletion in mouse Cmah increases disease severity in the mdx model of Duchenne muscular dystrophy. *Sci. Transl. Med.* **2,** 42ra54

45. Martin, P. T., Camboni, M., Xu, R., Golden, B., Chandrasekharan, K., Wang, C. M., Varki, A., and Janssen, P. M. (2013) *N*-Glycolylneuraminic acid deficiency worsens cardiac and skeletal muscle pathophysiology in α-sarcoglycan-deficient mice. *Glycobiology* **23,** 833–843

46. Valiente, O., Mauri, L., Casellato, R., Fernandez, L. E., and Sonnino, S. (2001) Preparation of deacetyl-, lyso-, and deacetyl-lyso-GM3 by selective alkaline hydrolysis of GM3 ganglioside. *J. Lipid Res.* **42,** 1318–1324

47. Palestini, P., Allietta, M., Sonnino, S., Tettamanti, G., Thompson, T. E., and Tillack, T. W. (1995) Gel phase preference of ganglioside GM1 at low concentration in two-component, two-phase phosphatidylcholine bilayers depends upon the ceramide moiety. *Biochim. Biophys. Acta* **1235,** 221–230

48. Yu, R. K., and Ledeen, R. W. (1972) Gangliosides of human, bovine, and rabbit plasma. *J. Lipid Res.* **13,** 680–686

49. Ando, S., Chang, N. C., and Yu, R. K. (1978) High-performance thin-layer chromatography and densitometric determination of brain ganglioside compositions of several species. *Anal. Biochem.* **89,** 437–450

50. Chisada, S., Yoshimura, Y., Sakaguchi, K., Uemura, S., Go, S., Ikeda, K., Uchima, H., Matsunaga, N., Ogura, K., Tai, T., Okino, N., Taguchi, R., Inokuchi, J., and Ito, M. (2009) Zebrafish and mouse α2,3-sialyltransferases responsible for synthesizing GM4 ganglioside. *J. Biol. Chem.* **284,** 30534–30546

51. Go, S., Sato, C., Yin, J., Kannagi, R., and Kitajima, K. (2007) Hypoxia-enhanced expression of free deaminoneuraminic acid in human cancer cells. *Biochem. Biophys. Res. Commun.* **357,** 537–542

52. Livak, K. J., and Schmittgen, T. D. (2001) Analysis of relative gene expression data using real-time quantitative PCR and the $2^{-\Delta\Delta CT}$ method. *Methods* **25,** 402–408

Altered expression of ganglioside GM3 molecular species and a potential regulatory role during myoblast differentiation

Shinji Go, Shiori Go, Lucas Veillon, Maria Grazia Ciampa, Laura Mauri, Chihiro Sato,
Ken Kitajima, Alessandro Prinetti, Sandro Sonnino and Jin-ichi Inokuchi

Access the most updated version of this article at doi: 10.1074/jbc.M116.771253

This article cites 52 references, 22 of which can be accessed free at
http://www.jbc.org/content/292/17/7040.full.html#ref-list-1